

# The Use of Magnetic Nanoparticles in Analytical Chemistry

Jacob S. Beveridge, Jason R. Stephens,  
and Mary Elizabeth Williams

Department of Chemistry, The Pennsylvania State University, University Park,  
Pennsylvania 16803; email: jsb332@psu.edu, jrs1089@psu.edu, mbw@chem.psu.edu

Annu. Rev. Anal. Chem. 2011. 4:251–73

First published online as a Review in Advance on  
March 15, 2011

The *Annual Review of Analytical Chemistry* is online  
at [anchem.annualreviews.org](http://anchem.annualreviews.org)

This article's doi:  
10.1146/annurev-anchem-061010-114041

Copyright © 2011 by Annual Reviews.  
All rights reserved

1936-1327/11/0719-0251\$20.00

## Keywords

sensors, imaging, separation, superparamagnetic, detection

## Abstract

Magnetic nanoparticles uniquely combine superparamagnetic behavior with dimensions that are smaller than or the same size as molecular analytes. The integration of magnetic nanoparticles with analytical methods has opened new avenues for sensing, purification, and quantitative analysis. Applied magnetic fields can be used to control the motion and properties of magnetic nanoparticles; in analytical chemistry, use of magnetic fields provides methods for manipulating and analyzing species at the molecular level. In this review, we describe applications of magnetic nanoparticles to analyte handling, chemical sensors, and imaging techniques.

## 1. INTRODUCTION

Nanomaterials have begun to revolutionize the world around us. Magnetic nanomaterials are unique because of their interactions with magnetic fields and field gradients, which enable the development of both fundamental experiments and applied products that exploit these magnetic behaviors. Emerging analytical techniques and new uses of conventional methods have begun to integrate magnetic nanoparticles to take advantage of the ability to magnetically induce motion, enhance signals, and switch behaviors. This review describes novel and broad uses of magnetic nanoparticles for analytical methodologies including (a) preconcentration, separation, and capture of analytes; (b) sensors and detection; and (c) imaging. Analysis of magnetic nanoparticle structure and properties, although related to our discussion, is a separate and equally broad topic that we do not address here.

The electrical, optical, and magnetic properties of materials can dramatically change as they are reduced from macro- to nanoscale dimensions. Integration of materials with biological species is particularly appealing because of these objects' relative dimensions (**Figure 1**). Taking advantage of the novel properties and favorable dimensions of nanomaterials is particularly meaningful in analytical techniques in which multiplexing, decreased analysis time, a large surface-to-volume ratio, and small environmental perturbation are desired.

Interest in magnetic nanoparticles has increased enormously over the past two decades. Fundamental research elucidating nanoparticle structure, physical and magnetic properties, and toxicity (among other characteristics) has led to the development of magnetic nanoparticles for industrial and biomedical applications. The magnetic properties of nanostructures allow one to control location and motion with externally applied magnetic fields; enable tracking and visualization of the local environment by use of magnetic resonance imaging (MRI); and yield, through magnetic tagging of molecules, a detection probe. Such advantages allow for control of the particle, and anything attached to it, that cannot be achieved otherwise. Most biological media have no naturally occurring magnetic component, which is advantageous when using magnetic nanoparticles in that they can be selectively controlled and/or detected with great specificity and low background noise.

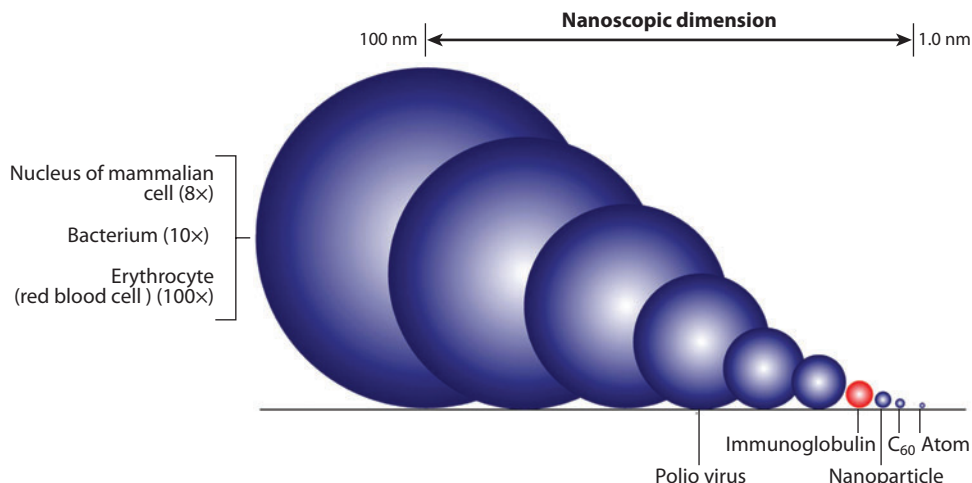


**Figure 1**

Size scale of some common biological and nano-objects. Reproduced from Reference 1 with permission from the Royal Society of Chemistry.

We briefly discuss the synthesis and magnetic properties of nanoparticles, including methods for functionalization, to provide a basic understanding of the types of materials that are available for analytical methods. The remainder of this review describes state-of-the-art uses of magnetic particles in analytical chemistry. Because this is a broad and quickly growing area, the reports we describe represent only a fraction of the available publications in this exciting and vigorous field.

---

**SQUID:**  
superconducting  
quantum interference  
device

---

## 2. NANOPARTICLE SYNTHESSES AND PROPERTIES

Many types of magnetic nanoparticles can be synthesized; these include iron oxides ( $\text{Fe}_2\text{O}_3$  and  $\text{Fe}_3\text{O}_4$ ); ferrites of cobalt, manganese, nickel, and magnesium; and FePt,  $\gamma\text{-Fe}_2\text{O}_3$ , cobalt, iron, nickel,  $\alpha\text{-Fe}$ , CoPt, and FeCo particles. FePt and CoPt nanoparticles are especially interesting because they are both magnetic and catalytic. The most commonly employed magnetic nanoparticles for analytical techniques tend to be  $\text{Fe}_3\text{O}_4$ ,  $\text{MnFe}_2\text{O}_4$ , and  $\text{CoFe}_2\text{O}_4$  because they are easy to synthesize with size-monodisperse products with high magnetic moments. Iron oxide is generally considered biocompatible and, thus, is the only nanoparticle material to have been approved by the U.S. Food and Drug Administration. Iron oxide nanoparticles also have the advantage of multiple synthetic routes for chemical functionalization. As a result, much of the following discussion focuses on iron oxide. The type of oxide, generally  $\text{Fe}_3\text{O}_4$  or  $\gamma\text{-Fe}_2\text{O}_3$ , is often not identified in the literature and can be difficult to distinguish in particles that are not single crystals. **Figure 2a–b** shows examples of transmission electron microscopy images of  $\text{Fe}_3\text{O}_4$  nanoparticles ranging from 6 to 13 nm in average diameter. These particles are spherical in shape and are notable for their narrow size distributions (i.e., they are size monodisperse).

When their diameter is less than  $\sim 30$  nm, magnetic nanoparticles are generally superparamagnetic, which means that they have no “magnetic memory.” In the absence of a magnetic field, superparamagnetic nanoparticles have no net magnetic dipole because thermal fluctuations cause the spins to randomly orient. However, when a magnetic field is applied to the nanoparticles, a magnetic dipole is induced. After the external magnetic field is removed, the magnetic nanoparticles randomly orient, and the nanoparticles return to their native nonmagnetic state. Superparamagnetism is measured with a superconducting quantum interference device (SQUID) magnetometer and is characterized by recording the magnetization–versus–applied magnetic field curve (**Figure 2i–k**). If the nanoparticles are superparamagnetic at room temperature, the curve reveals a saturation of the magnetization and no hysteresis around the origin, indicating that there is no magnetic memory (**Figure 2k**). Superparamagnetic properties are advantageous because the magnetic nanoparticles can be easily dispersed in solvent without attractive magnetic forces inducing aggregation. There is also no remnant magnetic field due to the magnetic nanoparticles, which is important for magnetic sensors. Superparamagnetism in nanoparticles is determined by the type of material, the crystallinity of the structures, and the particle’s size (i.e., number of spins). Therefore, there is no general rule that predicts the magnetic properties of a nanoparticle.

Magnetic nanoparticles are most commonly synthesized by one of three wet chemical routes: (a) high-temperature thermal decomposition and/or reduction, (b) coprecipitation, or (c) templated synthesis in the interior of micelles. Although they result in hydrophobic magnetic nanoparticles that require further chemical functionalization for biomedical applications, the high-temperature methods produce magnetic nanoparticles with better monodispersity and higher crystallinity. The  $\text{Fe}_3\text{O}_4$  particles (**Figure 2a–b**) were produced by high-temperature synthesis. This synthetic approach can easily be scaled up to produce large quantities of nanoparticles. Typical high-temperature syntheses begin with a metal precursor [such as  $\text{Co}(\text{acetylacetonate})$  or  $\text{Fe}(\text{CO})_5$ ], a reducing agent (such as 1,2-hexadecanediol or 1,2-tetradecanediol), stabilizing agent(s) (such as hexadecylamine or oleic acid/oleylamine), and a high-temperature boiling-point solvent (such as

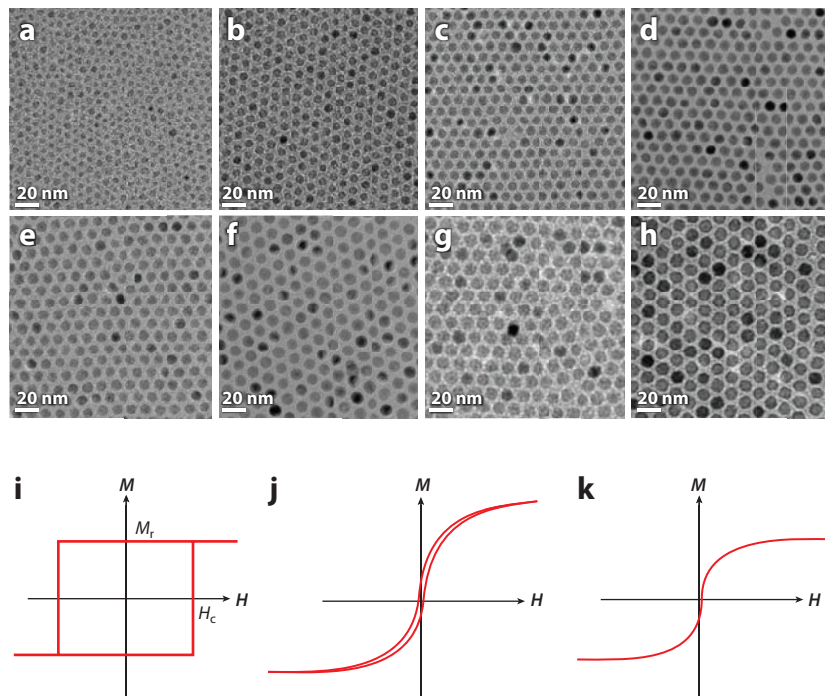


**Figure 2**

(*a–b*) Transmission electron microscopy images of size-controlled thermal decomposition synthesis of Fe<sub>3</sub>O<sub>4</sub>. The diameters of the particles in panels *a* through *b* range from 6 to 13 nm, respectively. Reproduced from Reference 5 with permission. Copyright 2004, Wiley. (*i–k*) Magnetization (*M*) versus applied magnetic field (*H*) curves of (*i*) a hard magnetic material, (*j*) a weak ferromagnetic material, and (*k*) a superparamagnetic material. Reproduced with permission from Reference 10. Copyright 2007, Wiley.

benzyl ether or octyl ether). Achieving a specific ratio of metal precursor to stabilizing agent is critical to obtain size-monodisperse nanoparticles. Similarly, the applied temperature affects the particles' resulting diameter and monodispersity.

Sun et al. (2) developed a synthetic route to produce metal (e.g., cobalt, iron, manganese) ferrite nanoparticles using metal acetylacetonate precursors and showed that larger particles could be prepared using small magnetic nanoparticles as seeds. Hyeon et al. (3) synthesized size-monodisperse iron oxide using Fe(CO)<sub>5</sub> or iron oleate (4) precursors; through an optimized method, the thermal decomposition of iron pentacarbonyl [Fe(CO)<sub>5</sub>] produced the iron oxide nanoparticles shown in **Figure 2a–b**. In this study, the authors achieved an unprecedented control over the diameter of Fe<sub>3</sub>O<sub>4</sub> particles (5). It was determined that the Fe(CO)<sub>5</sub> was responsible for nucleation and that the iron oleate was responsible for the growth of the iron oxide nanoparticles. Cobalt ferrite nanoparticles have also been synthesized using cobalt oleate and iron oleate reactants (6). In subsequent work, the mechanism for the oleate method of CoFe<sub>2</sub>O<sub>4</sub> synthesis was reported (7). Sun and colleagues (8) reported a robust synthesis of FePt in which Pt(acetylacetonate) and Fe(CO)<sub>5</sub> were used as metal precursors. Synthesis of FePt nanoparticles and FePt-Fe<sub>3</sub>O<sub>4</sub> heterodimer nanoparticles was also reported by Manna and coworkers (9).

The coprecipitation and microemulsion syntheses of magnetic nanoparticles use metal salts, rather than organometallic reagents, as precursors. Coprecipitation synthesis of magnetic

nanoparticles requires low temperatures and produces water-soluble magnetic nanoparticles. These advantages contrast sharply with the poor monodispersity (i.e., broad size distribution) and crystallinity of the product nanoparticles. Reaction parameters that affect the properties of the magnetic nanoparticles are the solution pH and temperature, the stirring or mixing rate, the anion of the salt, and the concentration of metal ions. Microemulsion or micelle synthesis, which is also performed in aqueous solutions, offers better monodispersity control compared with coprecipitation, but the range of nanoparticle diameters is limited by the size of the inverse micelle interior. As with coprecipitation, magnetic nanoparticles synthesized via microemulsion often suffer from poor crystallinity. A detailed discussion of magnetic nanoparticle syntheses, beyond the scope of this review, can be found elsewhere (10–14).

Magnetic nanoparticles must be stabilized by molecules attached to (i.e., ligands) or associated with (i.e., ions) their surfaces to prevent irreversible agglomeration and to enable dissolution. Magnetic nanoparticles synthesized through high-temperature routes are typically hydrophobic and can be functionalized by exchanging the surface ligands with others present in solution (15–17). Alternatively, association and encapsulation with a phospholipid, which forms a bilayer on the surface of the particle, have been used to make these particles water soluble and amenable for biological applications (18, 19). For many applications, the surface of the magnetic nanoparticles must be further derivatized to perform a function such as binding with a target, carrying a drug, and detecting an environment. Magnetic nanoparticles can be coated with a shell of another material, typically a thin layer of gold (20, 21), SiO<sub>2</sub> (22, 23), or carbon (24), so as to perform these chemical modifications and extend the range of methods available for functionalization. Encapsulation in a shell leads to the creation of particle heterostructures that (*a*) retain the magnetic properties of the magnetic nanoparticle core and (*b*) have surfaces that are amenable to modification through well-established methods.

### 3. PRECONCENTRATION, CAPTURE, AND SEPARATIONS

Magnetic nanoparticles are useful tools for the capture, concentration, and separation of many types of analytes from complex matrices. A plethora of work on superparamagnetic beads with microscale dimensions has been performed (25–28). Magnetic nanoparticles are advantageous for such analytical methods because they have a large surface-to-volume ratio, are comparable in size to many analytes of interest, are readily dispersible in solution, and have physical properties that are useful for enhancing signal detection. However, two challenges for the use of magnetic nanoparticles in analysis exist. First, large magnetic field gradients are needed to manipulate the magnetic nanoparticles because sufficient magnetic force must be exerted on the particles. Although the amount of magnetic force needed depends on the magnetic properties of the particle, the fields needed to move particles are typically  $\sim 100 \text{ T m}^{-1}$ , but they can be much larger. Second, although the use of magnetic nanoparticle surfaces for capturing analytes enables the concentration, separation, quantification, and further analysis of the analytes, the magnetic nanoparticles must first be functionalized with the appropriate chemistries. Below, we discuss research that addresses these challenges and demonstrates the use of magnetic nanoparticles in analytical methodologies.

Lin and colleagues (29) developed a technique known as nanoprobe-based affinity mass spectrometry (NBAMS) (Figure 3). In this technique, nanoparticles functionalized with capture probes are (*a*) used to bind a target analyte, (*b*) isolated, and (*c*) analyzed by mass spectrometry. Magnetic nanoparticles are ideal for use as the nanoprobes in NBAMS because they are easily separated and can be concentrated through application of a magnetic field.

The iron oxide magnetic nanoparticles used by Lin and colleagues were bifunctional: They served both as a solid laser desorption/ionization element and as a probe for the enrichment

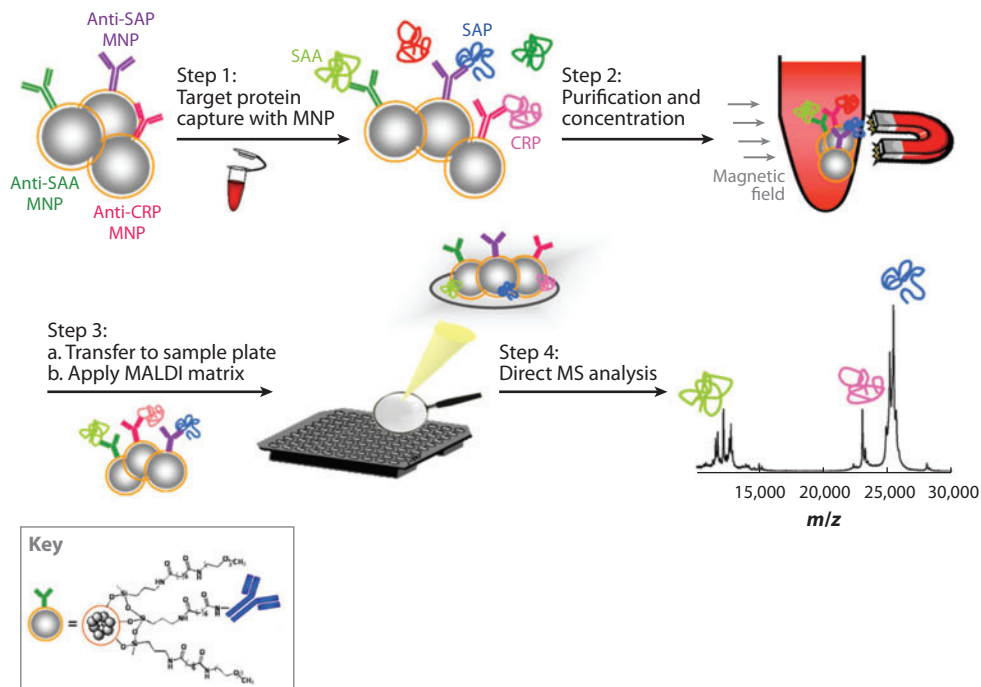


**Figure 3**

Role of the magnetic nanoparticle in a multiplexed immunoassay. The antibody-tagged magnetic nanoparticles (MNPs) capture the target; separate, purify, and concentrate the target; and act as a platform for the analysis of the target by matrix-assisted laser desorption/ionization (MALDI) time-of-flight mass spectrometry (MS). Abbreviations: CRP, C-reactive protein; SAA, serum amyloid A; SAP, serum amyloid P. Reproduced with permission from Reference 32. Copyright 2005, Wiley.

and extraction of the small-molecule targets from a complex solution (e.g., blood serum) (30). The target, bound to the magnetic nanoparticle, was subsequently identified with matrix-assisted laser desorption/ionization mass spectrometry. This technique was cost-effective and could be automated to screen the small molecules salicylamide, mefenamic acid, ketoprofen, flufenamic acid, sulindac, prednisolone, and mannose from blood serum. Chen et al. (31) used NBAMS to perform an immunoassay to identify proteins (**Figure 3**). These authors utilized antibody-conjugated iron oxide nanoparticles to capture target proteins and separate them from their matrix for analysis by mass spectrometry (31, 32). The capture efficiency and the detection specificity of the proteins on magnetic nanoparticles and on superparamagnetic microbeads were compared. The performance of the magnetic nanoparticles was superior in both cases.

In another study (33), mass spectrometry was used to identify viruses captured by alumina-coated Fe<sub>3</sub>O<sub>4</sub> nanoparticles. To develop a more general method to bind protein to magnetic nanoparticles, Chen et al. (34) placed a nitrilotriacetic acid (NTA) derivative on the surface of ~50-nm-diameter iron oxide nanoparticles. NTA chelated the transition-metal ions Ni(II), Zr(IV), and Gd(III), and each magnetic nanoparticle–NTA–metal ion complex targeted the capture of a specific protein. Following capture of the target protein, the magnetic particle structure was separated and analyzed by mass spectrometry. In more recent work, Xie et al. (35) used Fe<sub>3</sub>O<sub>4</sub>-gold core-shell nanoparticles functionalized with NTA to complex Ni(II) for use as a

**NTA:** nitrilotriacetic acid

selective histidine adsorbent. These magnetic nanoparticle structures were used to extract, purify, and concentrate histidine-tagged proteins.

Magnetic nanoparticles have also been used to concentrate samples in microfluidic chips. Chen et al. (36) created a microfluidic magnetic separator chip, which they used to concentrate human immunodeficiency virus (HIV) from plasma. The authors used superparamagnetic nanoparticles conjugated to anti-CD44 (developed by Miltenyi Biotec) to capture the virus, then passed the particles through a packed bed of 25–75- $\mu\text{m}$ -diameter iron oxide particles. An external magnet was used to magnetize the packed bed, which caused the HIV–magnetic nanoparticle conjugates to be trapped, thereby separating and concentrating them from the plasma matrix. Off-chip enzyme-linked immunosorbent assay confirmed that the HIV virions were concentrated by a factor of approximately 80-fold over the original solution.

Immunoassays using magnetic nanoparticles have also been performed. For example, Furlong and colleagues (37) used magnetic nanoparticles to detect staphylococcal enterotoxin B: Antibody-functionalized magnetic nanoparticles (Miltenyi Biotec  $\mu\text{MACS}^{\text{®}}$ ) captured the enterotoxin antigen from solution, isolated it via magnetic separation, and amplified the surface plasmon resonance (SPR) signal for the antigen. Through the use of this approach, a limit of detection of less than 100  $\text{pg ml}^{-1}$  was reached. The multiple uses of magnetic nanoparticles in this assay highlights their utility for analyses.

Carbon nanotubes (CNTs) decorated with magnetic nanoparticles have also been used for the capture of small molecules. Schmitt-Kopplin and colleagues (38) found that the percent recovery during capture of (fluoro)quinolones was more efficient for CNT-magnetic nanoparticle heterostructures than for either of the unlinked individual species. In these assemblies, the CNT enhanced adsorption, and the magnetic nanoparticle enabled magnetic separation and concentration of these drugs from human plasma samples.

Magnetic nanoparticles have been applied to environmental cleanup and the analysis of natural water. Ballesteros-Gómez & Rubio (39) performed a solid-phase extraction of carcinogenic polycyclic aromatic hydrocarbons from water samples. Hemimicelles of tetradecanoate surrounding 20–30-nm-diameter iron oxide nanoparticles were used to capture and concentrate the hydrocarbons. Because of the highly efficient capture by the magnetic nanoparticles, the extractant required no additional purification; this observation was verified through liquid chromatography with fluorescent detection. This method's limit of quantification was 0.2–0.5  $\text{ng liter}^{-1}$ —well below the allowable concentration in water. Additional research with magnetic solid-phase extraction has employed magnetic nanoparticles coated with silica or charcoal (40), polymers (41), and hemimicelles (42). These solid phases adsorbed organic dyes and phenolic compounds from aqueous samples.

To demonstrate the use of magnetic nanoparticles in biodefense applications, Bromberg et al. (43) functionalized iron oxide nanoparticles with polyethyleneimine surfactant with poly(hexamethylene biguanide), a broad-range antiseptic. These nanoparticles killed bacteria, viruses, and fungi. Following exposure to the sample, the 6-nm-diameter iron oxides formed  $\sim 60$ -nm-diameter clusters, which were then separated and concentrated using a high-gradient magnetic field separator. DNA from the captured species was identified via quantitative polymerase chain reaction.

Separations that use magnetic nanoparticles are important for the efficient analysis of molecules attached to nanoparticle surfaces. The most basic magnetic nanoparticle separations utilize a permanent magnet held against the wall of the container until the magnetic nanoparticles aggregate from the solution. Although this method is easy and inexpensive, the low-magnetic field gradients of handheld magnets can make the separation time-consuming and inefficient, particularly when the magnetic nanoparticles are well dispersed and stable in solution. For these reasons, researchers have focused on developing separation techniques for magnetic nanoparticles; two of

---

**HIV:** human immunodeficiency virus

**SPR:** surface plasmon resonance

**DNA:** deoxyribonucleic acid

---

**Table 1** Comparison between some properties of magnetic nanoparticle separations via column-flow mechanisms or in microfluidic chips

Comparison between magnetic nanoparticle separation techniques	
Column flow	Microfluidic devices
Low-magnetic field gradients	High-magnetic field gradients
High throughput	Low throughput
Soft magnetic packing often used	Open-channel or regularly patterned capture elements
Irregular flow paths	Predictable flow patterns
Analyte losses	Generally higher capture and elution efficiency
Forcible elutions occasionally needed	

the predominant separation techniques are compared in **Table 1**. Nishijima and colleagues (44) captured 6-nm-diameter FePt particles and 15-nm-diameter Fe<sub>3</sub>O<sub>4</sub> particles in a magnetic filter column. This column magnetically trapped magnetic nanoparticles on a packed bed of 0.3-mm ferromagnetic beads, which were magnetized by an external superconducting magnet. The magnetic nanoparticles were subsequently released into the eluent when the magnet was turned off. The authors achieved separation efficiencies of ~94% and 40% for Fe<sub>3</sub>O<sub>4</sub> and FePt, respectively.

Our group (45) separated different types (6-nm-diameter  $\gamma$ -Fe<sub>2</sub>O<sub>3</sub> and 13-nm-diameter CoFe<sub>2</sub>O<sub>4</sub>) of magnetic nanoparticles in open tubular capillary columns by use of magnetic field flow fractionation. More recently, we developed a differential magnetic catch-and-release (DMCR) method to separate different-sized magnetic nanoparticles (46). A polydisperse mixture of <20-nm-diameter CoFe<sub>2</sub>O<sub>4</sub> nanoparticles was magnetically trapped in an open tubular capillary column; changing the applied magnetic field gradient allowed monodisperse fractions to be selectively released into the flow stream. In the future, such separations may be applied to the simultaneous magnetic capture and separation of tethered biomolecules. In addition to the separation of the magnetic nanoparticles, magnetic and fluid drag equations were used to approximate the magnetic moments of the magnetic nanoparticles (46). **Figure 4** illustrates the capability of DMCR to separate magnetic nanoparticles. The CoFe<sub>2</sub>O<sub>4</sub> nanoparticles shown in **Figure 4d** have polydisperse diameters; these particles were separated into monodisperse fractions (**Figure 4a-c**) through the use of DMCR. The resolution between the magnetic nanoparticle peaks can be controlled by varying the strength of the magnetic field over time (**Figure 4e**) (J.S. Beveridge & M.E. Williams, unpublished observations).

Williams and colleagues (47) designed a variation of magnetic field flow fractionation by placing the separation channel in a quadrupole magnet geometry. Use of the quadrupole magnet revealed that the distributions of commercially supplied iron oxide nanoparticles were between 75 nm and 390 nm in diameter. This technique was sufficiently sensitive to discriminate between different manufactured lots of the same magnetic nanoparticles (48). In another study, Earhart et al. (49) fabricated a magnetic nanoparticle-trapping sifter, which was a membrane with slot-shaped pores on a Si<sub>3</sub>N<sub>4</sub> support. The pores were lined with a soft magnetic material (namely CoTaZr), which was magnetized in the presence of a magnetic field, trapping magnetic nanoparticles moving through the membrane. Capture efficiencies for the magnetic sifter ranged from 28% to 37% for 50-nm-diameter iron oxide nanoparticles.

High-gradient magnetic separations (HGMS), which are used predominantly for industrial processes, have begun to be applied as an analytical method used in conjunction with magnetic nanoparticles. In HGMS, a packed bed of soft magnetic steel wool or wire mesh within a column is placed into a uniform magnetic field. The packing in the column distorts the magnetic field lines, causing high local magnetic field gradients and allowing the capture or retention of the

**HGMS:** high-gradient magnetic separations



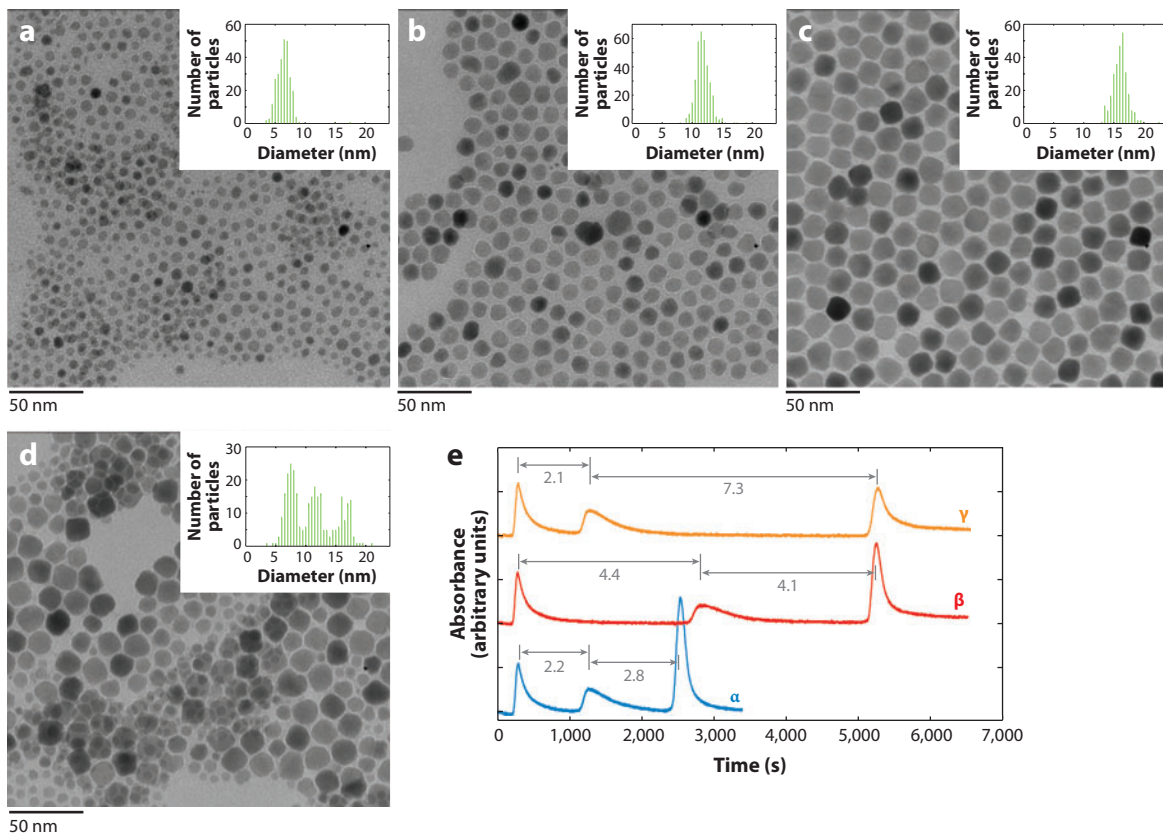


**Figure 4**

(*a–c*) Transmission electron microscopy images of monodisperse fractions of  $\text{CoFe}_2\text{O}_4$  nanoparticles that were separated from a polydisperse nanoparticle mixture (*d*). (*Insets*) The diameter distribution of the nanoparticles shown in each panel: (*a*) 7 nm, (*b*) 11 nm, and (*c*) 17 nm. (*e*) Three chromatograms ( $\alpha$ ,  $\beta$ ,  $\gamma$ ) of the separation in panel *d*, showing the control in resolution between nanoparticle peaks (*gray*).

magnetic nanoparticles that pass over the bed. Although much of the HGMS literature focuses on micrometer-sized particles, multiple theoretical simulations predict the separation of magnetic nanoparticles in an HGMS apparatus (50–52). Hatton and colleagues (53) experimentally studied the feasibility of capturing magnetic nanoparticles from water via HGMS. The authors' samples of 7.5-nm-diameter iron oxide nanoparticles were individually functionalized with either a phospholipid or a polyacrylic acid–polyethylene oxide and polypropylene oxide copolymer. Although HGMS did not capture individual particles, aggregates of the iron oxide–copolymer and the iron oxide–phospholipid nanoparticles were trapped. Subsequent research focused on the HGMS of magnetic nanoclusters; clusters with diameters greater than 50 nm were trapped efficiently, even at high flow rates (54).

#### 4. SENSORS AND DETECTION

The use of magnetic sensors for bioanalysis is advantageous because most biological species are not magnetic, which means that there is inherently low background noise. Magnetic sensors are

---

**GMR:** giant magnetoresistive

**MTJ:** magnetic tunnel junction

---

therefore very sensitive to magnetically labeled species. Magnetic sensors can be integrated into microfluidic chips, often provide an electronic signal readout, are inexpensive to fabricate, and can employ magnetic labels that are commonly used in bioassays. A particular advantage of magnetic nanoparticles is that their size is comparable to that of the biomolecule, whereas microbeads are orders of magnitude larger. Conjugating a nanoparticle to a biomolecule therefore causes less steric hindrance and enables the biomolecule to interact with the environment in a less obstructed way.

Three common magnetic sensors used to detect magnetic nanoparticles are (a) giant magnetoresistive (GMR) sensors, (b) magnetic tunnel junction (MTJ) sensors, and (c) SQUID sensors. Compared with SQUID sensors, GMR sensors are simpler and more portable, and they operate at room temperature. Although MTJ sensors have higher magnetoresistive sensitivity and can detect as few as 15 14-nm-diameter cobalt nanoparticles (55), they are still in an early phase of development compared with GMR sensors, and relatively few articles describe the use of MTJ sensors in conjunction with magnetic nanoparticles for analytical purposes (56, 57). For these reasons, we focus on GMR sensors and their applications to magnetic nanoparticles in analytical chemistry.

#### 4.1. Giant Magnetoresistive Sensors

Magnetoresistance is a property of some magnetic materials in which the electrical resistance changes in the presence of an applied magnetic field. Giant magnetoresistance occurs when such magnetoresistive ferromagnetic materials are reduced to nanometer-thick films and stacked with nonmagnetic layers. The 2007 Nobel Prize in Physics was awarded to Fert and Grünberg for the discovery and explanation of the underlying physics of giant magnetoresistance (see References 58 and 59).

GMR spin-valve sensors are highly sensitive to magnetic fields and can detect the stray field of a magnetically excited superparamagnetic particle. Although most of the literature focuses on the detection of biomolecules tagged with micrometer- or submicrometer-sized superparamagnetic beads, Wang and colleagues (60) posit that magnetic nanoparticles are preferable for analytical detection. An array of submicrometer-sized GMR spin-valve-based sensors detected fewer than 50 16-nm-diameter  $\text{Fe}_3\text{O}_4$  nanoparticles. As illustrated in **Figure 5**, the small size of spin-valve sensors allows them to be easily integrated into microfluidic chips (61). Wang et al. (62) integrated a GMR sensor into a microfluidic chip to rapidly perform a DNA assay in less than 1 h and with detection limits near 10 pM. The Wang group's research suggests that if this technique were optimized, the detection limit could be improved to 1 pM or lower (62).

Using a GMR sensor, investigators have demonstrated human papillomavirus genotyping in a microfluidic chip (63). We direct interested readers to an excellent and comprehensive review of both GMR sensors and the use of spin-valve sensors to detect magnetic nanoparticle-tagged biomolecules (64).

#### 4.2. Electrochemical Sensors

Because of their ability to enhance electrochemical signals, magnetic nanoparticles have been integrated into electrochemical sensors. Such integration can be accomplished in three ways: (a) through contact between the metallic magnetic nanoparticle and the electrode surface, (b) through transport of a redox-active species to the electrode surface, or (c) through formation of a thin film on the electrode surface, which increases the surface area and modifies its performance. Amperometry, potentiometry, stripping analysis, cyclic voltammetry, and impedance spectroscopy, together with magnetic nanoparticles, have been used for electrochemical detection.

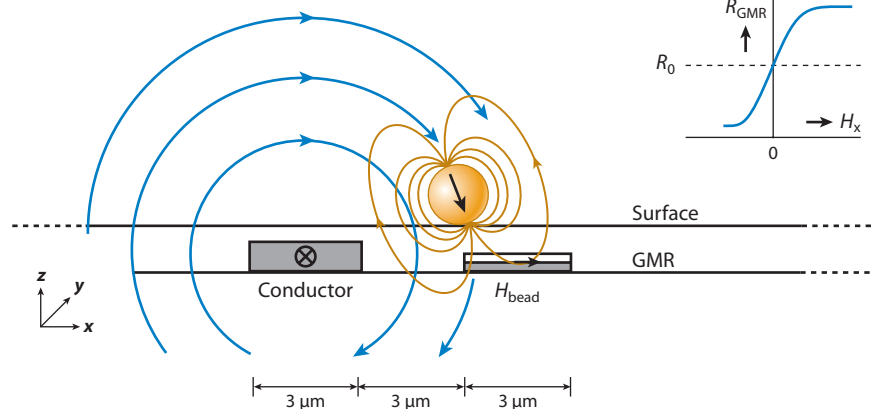


**Figure 5**

Cross section of a giant magnetoresistive (GMR) sensor with a magnetic nanoparticle label on the sensor surface. An excitation current flowing through the integrated conductors produces the excitation field. The stray field from the magnetic nanoparticle that is magnetized by the excitation field leads to a resistance variation in the GMR sensor. Reproduced with permission from Reference 61. Copyright 2007, the American Chemical Society.

Hirsch et al. (65) reported the first magnetically switchable electrode in which the electrochemical reaction could be turned on or off, depending on the magnetic particles' response to the magnetic field orientation. Although this initial study used micrometer-sized magnetic particles, subsequent studies employed iron oxide nanoparticles to perform similar "on/off" electrochemistry. For example, hydrophobicity and hydrophilicity can be magnetically controlled at the electrode surface by the movement of the nanoparticles (**Figure 6**) (66). In this experiment, the electrochemical cell was composed of (a) a gold electrode with an aqueous buffer and (b) an organic solvent bilayer electrolyte located above the electrode. When a magnetic field was applied, hydrophobic magnetic  $\text{Fe}_3\text{O}_4$  nanoparticles were pulled from the upper organic layer into the aqueous layer, forming a membrane-like film on the electrode surface and inhibiting the electrochemistry at the electrode to create the "off" state. Blocking of electron transfer at the electrode was examined via Faradaic impedance spectroscopy. The redox current was restored to the "on" state by placing the magnet above the organic phase, which pulled the magnetic nanoparticles into the upper organic layer and allowed oxidation of the redox probe (e.g., ferrocene dicarboxylic acid) at the unblocked electrode. Larger (>200-nm-diameter) magnetic particles did not effectively block the electrode surface; this finding was attributed to pinhole defects between the particles that allowed the redox probe to diffuse to the electrode surface. Further experiments using quinones immobilized on the electrode demonstrated switchable aqueous and organic redox mechanisms at the electrode surface (67). Blockage of a bioelectrocatalytic reaction was demonstrated by immobilizing ferrocene on an electrode surface: The oxidation of glucose by glucose oxidase was controlled with magnetic fields applied to manipulated nanoparticles and the electrode function (67). The same investigators used magnetic nanoparticles to deliver a redox-active species to the electrode surface by adsorbing cumene hydroperoxide to the magnetic nanoparticles and using the particles' magnetic motion to transport the redox-active cumene to the electrode (67).

Photoelectrochemical currents can be magnetically controlled with electrode-bound quantum dots (68). Also, DNA hybridization, biocatalytic replication, and digestion can be controlled when magnetic nanoparticles are directed to and from the electrode surface (69). Similarly, oleic

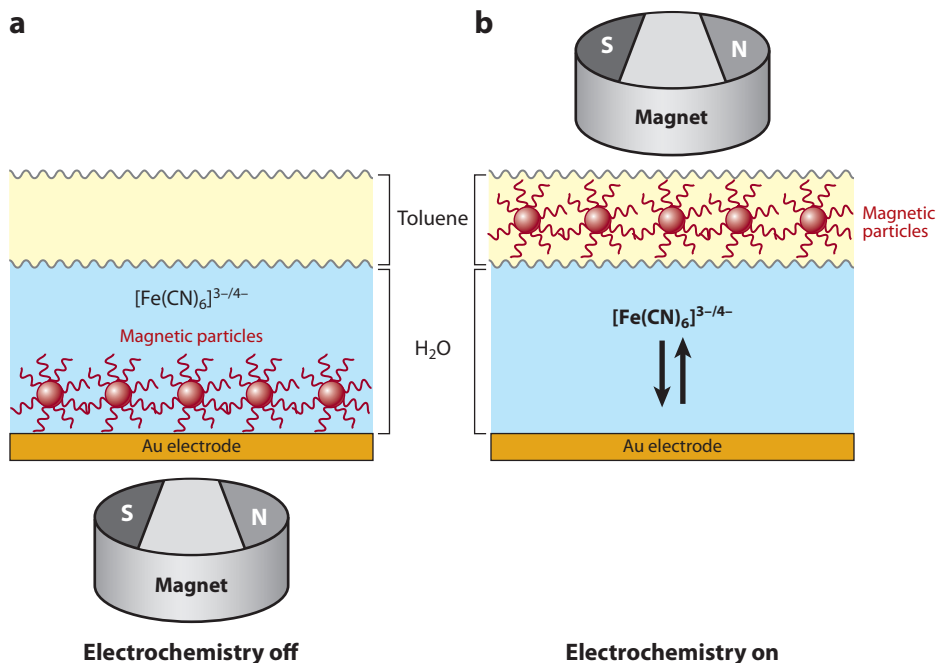


**Figure 6**

Magnetocontrolled switchable electrode via translocation of functionalized magnetic nanoparticles. (a) A magnet placed below the electrode pulls the magnetic nanoparticles into the aqueous phase, and the magnetic nanoparticles form a layer on the electrode surface. (b) A magnet placed above the electrode returns the magnetic nanoparticles to the organic phase, revealing the electroactive species to the electrode surface. Reproduced with permission from Reference 66. Copyright 2004, the American Chemical Society.

acid-coated magnetic iron oxide nanoparticles can be used to either block or allow the hybridization of DNA on an electrode surface (70).

Small-molecule detection on magnetic nanoparticle-modified carbon paste electrodes has been demonstrated. In these experiments, magnetic nanoparticles are modified with a catalyst and held against the electrode surface with a magnet. With the magnet in place, particles containing catalyst react, and the products are electrochemically detected. Liu et al. (71) constructed a phenol biosensor using tyrosinase-modified magnetic nanoparticles, and Li et al. (72) used Prussian blue and glucose oxidase to modify magnetic nanoparticles for a sensitive glucose sensor. One of the main advantages of magnetic nanoparticle catalyst-modified electrodes is the ease of renewing the biocatalyst on the surface: By releasing the field and replacing it with new magnetic nanoparticles, a fresh catalytic electrode surface can easily be generated.

Antigens and cysteine have been attached to magnetic nanoparticles for a sandwich immunoassay to detect human immunoglobulin G on carbon paste electrode-supported magnetic nanoparticles (73, 74). The advantages of such electrochemical sensors include their simple construction, magnetic manipulation, and low cost. Carbon paste electrodes with magnetic nanoparticles have also been used to detect lead in urine and heavy metals in water. Yantasee et al. (75) used dimercaptosuccinic acid-functionalized 20-nm-diameter  $\text{Fe}_3\text{O}_4$  nanoparticles on carbon paste and glassy carbon electrodes to detect lead in urine and copper, lead, cadmium, and silver in natural water. This technique has a limit of detection lower than 1 ppb, as well as the potential to be fully automated via an electromagnet.

In another experiment, an immunoassay was performed on 100-nm-diameter  $\text{Fe}_3\text{O}_4$  nanoparticles that were linked to  $\text{SiO}_2$  beads, via a sandwich-type assay, for electrochemical signal enhancement (76). The immunoassay was performed in a flow cell in which the magnetic nanoparticles acted as anchors. First, analytes were injected into the cell, where they reacted with the magnetic nanoparticles, and were magnetically trapped against the electrode for detection by measurement of the impedance. Then, the electrode was regenerated in the flow cell through removal of the magnetic field and subsequently trapping of new particles. The linear range of this method was greater than that of competing techniques, and it had a lower or equivalent limit of detection. In an analogous study, a flow cell was used to renew the carbon paste electrode in a magnetocontrolled immunoassay (77).

CNTs can be used on electrodes because of their high electrocatalytic activity and fast electron transfer. Zhang et al. (78) employed magnetic nanoparticle-decorated CNTs covalently immobilized on a gold electrode. The investigators observed exceptional electrocatalytic activity of the  $\text{Fe}_3\text{O}_4$  nanoparticle-CNT electrode for the oxidation of catechol, along with enhanced redox peak currents of catechol on the magnetic nanoparticle-CNT electrode, which were attributed to the larger surface area and the promotion of electron transfer. Magnetic nanoparticles combined with CNTs have also been used for the electrochemical detection of glucose and DNA (79–81).

Detection of gas-phase analytes has been performed by monitoring the changes in resistance of an iron oxide-polypyrrole nanoparticle composite (82). In this experiment,  $\text{Fe}_3\text{O}_4$  nanoparticles and polypyrrole particles were combined in a heterogeneous mixture that was copolymerized. The resulting dry powder was pressed into a pellet; silver electrodes were attached to the pellet; and the resistance between the electrodes was measured in the presence of water and  $\text{N}_2$ ,  $\text{O}_2$ , and  $\text{CO}_2$  for the detection of these gases. Gas detection has also been investigated with submicrometer- to micrometer-sized iron oxide particles (83, 84).

### 4.3. Colorimetric Sensors

Gao et al. (85) found that magnetite nanoparticles possess intrinsic peroxidase activity—an unexpected observation, given that  $\text{Fe}_3\text{O}_4$  nanoparticles had been commonly believed to be chemically inert. The catalytic activity of the  $\text{Fe}_3\text{O}_4$  nanoparticles was characterized and compared with that of horseradish peroxidase. In the immunoassay, the magnetic nanoparticles performed three functions: capture, separation, and detection. Wei & Wang (86) used the peroxidase activity of  $\text{Fe}_3\text{O}_4$  nanoparticles for the colorimetric detection of hydrogen peroxide and glucose. The ability of  $\text{Fe}_3\text{O}_4$  nanoparticles to detect  $\text{H}_2\text{O}_2$  was exploited for the colorimetric detection of melamine in milk products (87). This detection system was sensitive and selective, as well as visually verifiable.

### 4.4. Optical Sensors

Magnetic nanoparticles have been used for the detection of proteins in bead assays monitored by optical microscopy. Fuh and colleagues (88) magnetically trapped antigen-functionalized  $\text{Fe}_3\text{O}_4$  nanoparticles in a flow cell and used them to capture protein-labeled silica microbeads. The amount of protein was quantitatively determined, via optical microscopy, by counting the micrometer-sized silica beads. Magneto-optical relaxation has also been used to perform a liquid immunoassay in which magnetic nanoparticles were functionalized with antibody via streptavidin-biotin conjugation. Introduction of the protein antibody induced aggregation, the extent of which depended on the protein concentration and was detected magneto-optically (89).

#### 4.5. Other Sensors

Various types of nanoparticles have been employed to enhance SPR signals, and magnetic nanoparticles have also been used for enhanced SPR detection of biomolecules. Zhou and colleagues (90) described an indirect competitive inhibition assay to detect adenosine; these authors used magnetic nanoparticles to capture, purify, separate, and enrich the analyte, as well as to amplify the SPR signal.

Surface-enhanced Raman spectroscopy (SERS) has also benefited from the incorporation of magnetic nanoparticles through the development of M-SERS dots. M-SERS dots integrate a Fe<sub>3</sub>O<sub>4</sub> magnetic component into SERS dots, which are typically composed of a support particle (silica), a Raman-active chemical (such as 4-mercaptotoluene or thiophenol), and Ag nanoparticles. M-SERS dots have been used to isolate (through magnetic separation) cancer cells that were otherwise challenging to separate (91, 92).

Similar to the immobilization of magnetic nanoparticles onto electrodes, magnetic nanoparticles have been immobilized onto piezoelectric surfaces. Immunoassays performed on magnetic nanoparticle-modified surfaces use the sensitive mass detection of the piezoelectric device to monitor biomolecule capture during the assay. This approach represents a promising immunosensor with a renewable analysis surface and very low limits of detection (93).

Diagnostic magnetic resonance biosensors that utilize magnetic nanoparticles offer a promising point-of-care technique (94, 95). Magnetic resonance assays have been performed on small molecules as well as on biological species such as DNA, RNA, proteins, enzymes, cells, and organisms. Weissleder and colleagues (96) recently published a comprehensive review of this technique.

### 5. MAGNETIC RESONANCE IMAGING

Rather than utilizing small molecules such as gadolinium complexes as contrast agents, MRI can employ superparamagnetic nanoparticles. Magnetic nanoparticles remain in blood circulation longer, provide higher sensitivity because of their larger number of spins, and may have fewer adverse side effects (97).

Iron oxide is the most prevalent magnetic nanoparticle used for MRI largely because it is generally believed to be biocompatible. As of 2010, iron oxide is the only magnetic nanoparticle with U.S. Food and Drug Administration approval. MRI performed with superparamagnetic iron oxide nanoparticles *in vivo* has reached nearly microscale resolution (98). As a  $T_2$  (i.e., negative) contrast agent, iron oxide nanoparticles coated with dextran were first used to image the liver; later, they were used to image structures ranging from organs to cells. The dextran coating on iron oxide nanoparticles can be functionalized to enable specific targeting of cells or to contain a general transfection agent that allows nonspecific targeting. Josephson et al. (99) functionalized 41-nm-diameter iron oxide nanoparticles with a *trans*-activating transcriptional peptide that—in three cell lines—enabled an uptake efficiency of the magnetic nanoparticles that was 100 times greater than previously reported. Functionalization of the magnetic nanoparticle also determines where it accumulates within the cell (e.g., within the vesicles or the nucleus). Weissleder et al. (100) used dextran-coated magnetic nanoparticles and covalently attached human holotransferrin. These functionalities allowed the authors to monitor transgene expression *in vivo* using MRI; this research may have important implications for the monitoring of gene therapy via MRI.

Dextran-coated magnetic nanoparticles functionalized to target the transferrin receptor have been used to track cells responsible for the remyelination of axons in rats. In this experiment,

Bulte et al. (101) loaded CG-4 cells, which are myelinating cells, with magnetic nanoparticles. The remyelination of axons was tracked with MRI.

Conjugation of biomolecules on the surface of magnetic nanoparticles has been used to target both organs and specific cell lines. Using 6-nm-diameter  $\gamma$ - $\text{Fe}_2\text{O}_3$  particles coated with maleimide-functionalized phospholipid, which provides a route for the attachment of antibodies, O'Brien and colleagues (102) showed that the magnetic nanoparticle contrast agent could be targeted to cell receptors, specifically major histocompatibility class II receptors, which are prevalent in the medulla of the kidney.

Targeting and detection of cancerous cells are areas of interest for MRI of magnetic nanoparticles. MRI of iron oxide nanoparticles functionalized with carbohydrates is effective for the detection of cancerous cells. For example, Huang and colleagues (103) used a series of five different carbohydrates to functionalize magnetic nanoparticles. These authors determined the binding and selectivity of the magnetic nanoparticles' interaction with the carbohydrate receptors on the cells from the extent of MRI contrast and  $T_2$  relaxation times. This research showed that cell lines can be differentiated through the statistical method of linear discriminant analysis, that cancerous cells can be selectively detected, and that isogenic cell lines can be distinguished from one another.

Apoptosis of cancerous cells due to administration of a chemotherapy agent has also been monitored through the use of MRI. Brindle and colleagues (104) functionalized dextran-coated iron oxide nanoparticles with synaptotagmin I, whose  $C_2$  domain binds to the plasma membrane of apoptotic cells. These magnetic nanoparticle conjugates were injected into a mouse in which a cancerous tumor had previously been treated with a chemotherapeutic agent. The magnetic nanoparticles had a reduced signal at the site of the tumor, which indicated cell death. This type of detection is an especially promising technique to determine the effectiveness of chemotherapeutic treatment, as well as to monitor transplanted organs.

Unfunctionalized hydrophobic iron oxide nanoparticles have been utilized in *in vivo* MRI studies. The Bruns group (105) encapsulated magnetic nanoparticles in the lipid core of micelles. Hydrophobic iron oxide nanoparticles trapped in a liposome were subsequently used to quantitatively analyze the uptake and metabolism of the lipoproteins via MRI (106).

Although magnetic nanoparticles have been utilized as a contrast agent in MRI, radiolabeled nanoparticles can be used in positron emission tomography (PET), and plasmonic nanoparticles can be used in optical imaging. A current trend in biomedical imaging is the integration of these functional particles to produce a multifunctional nanostructure that enables an array of imaging techniques. Superparamagnetic iron oxide nanoparticles are  $T_2$  (i.e., dark signal)-weighted contrast agents, whereas paramagnetic small-molecule complexes containing  $\text{Gd}^{3+}$  or  $\text{Mn}^{2+}$  are  $T_1$  (i.e., bright signal)-weighted contrast agents. Park and colleagues (107) designed  $\text{Fe}_3\text{O}_4$  nanoparticles decorated with  $\text{Gd}^{3+}$  ions to create dual  $T_1$  and  $T_2$  magnetic resonance contrast agents. By use of dopamine as an anchor to the  $\text{Fe}_3\text{O}_4$  surface, the magnetic nanoparticles can be stabilized by a mixed layer of poly(ethylene glycol) (PEG) for solubility and chelating agents for the capture of  $\text{Gd}^{3+}$ .

The Park group compared the signals obtained during MRI of a rat with gadolinium-functionalized magnetic nanoparticles and the commercially available contrast agents Magnevist<sup>®</sup> and Feridex<sup>®</sup> (Figure 7). The authors' data demonstrate that these nanoparticles act as dual contrast agents.

Pichler and colleagues (108) multiplexed PET with MRI, a combination that provides complementary diagnostic information. The Bao group (109) recently developed a dual magnetic and radiolabel tracer within the same nanostructure to allow simultaneous PET and MRI with the same agent. In this case, magnetic resonance contrast arose from a 6.2-nm-diameter superparamagnetic iron oxide nanoparticle core coated with PEG micelles. Some of the PEG molecules

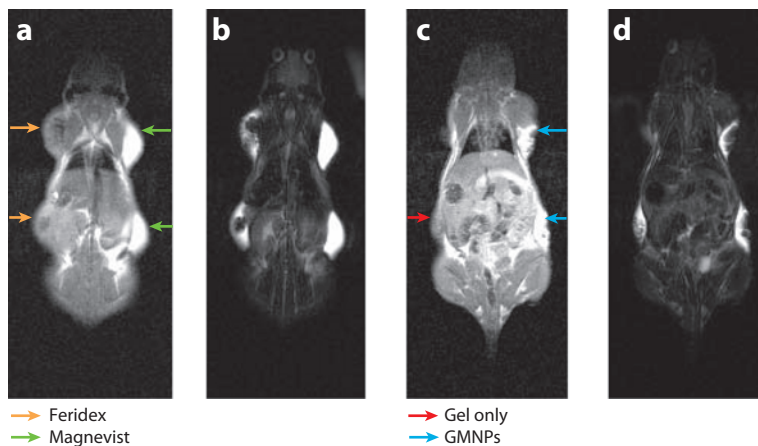


**Figure 7**

(a)  $T_1$ -weighted and (b)  $T_2$ -weighted magnetic resonance images of a mouse injected with Feridex<sup>®</sup> and Magnevist<sup>®</sup>. (c)  $T_1$ -weighted and (d)  $T_2$ -weighted magnetic resonance images of a mouse injected with gadolinium magnetic nanoparticles (GMNPs) and the hydrogel solution used as a control. Reproduced with permission from Reference 107. Copyright 2010, American Chemical Society.

were functionalized with tetraacetic acid, which was used to chelate  $^{64}\text{Cu}$  upon incubation. The biodistribution of these imaging agents was evaluated by PET and MRI both in vitro and in vivo. Several other examples of nanoparticles being used as dual imaging agents for PET and MRI have been reported (110–112).

Nanoparticles designed to multiplex optical imaging and MRI have also been investigated. Labhasetwar and colleagues (113) designed dual optical and MRI nanoparticle agents in which hydrophobic, oleic acid-coated  $\text{Fe}_3\text{O}_4$  nanoparticles with diameters between 10 and 25 nm were rendered hydrophilic by association with Pluronic<sup>®</sup> F127. Incubation of these particles with hydrophobic near-infrared fluorescence dyes (e.g., SDB5700, SDA5177, SDA6825, and Sdb5491) caused the dyes to be trapped in the oleic acid layer on the surface of the magnetic nanoparticles, yielding only very slow leakage over time in aqueous environments. Incorporation of the dyes enabled fluorescence imaging of the nanoparticles, and the magnetic component served both as an MRI contrast agent and as a magnetic field-induced accumulation agent at the tumor site.

Fluorescent dye molecules such as fluorescein isothiocyanate (99, 114), Texas Red (115), and Cy5.5 (116, 117) have also been conjugated to dextran- and phospholipid/PEG-stabilized  $\text{Fe}_3\text{O}_4$  nanoparticles to serve as dual optical/MRI probes. Magnetic nanoparticles are often coated with silica to reduce the fluorescence quenching of the dye emission by the nanoparticle. For example, Liong et al. (118) used silica-coated iron oxide nanoparticles to anchor fluorescein isothiocyanate and create a fluorescent magnetic nanoparticle. Similarly, Perez and colleagues (119) used a poly(acrylic acid) shell on the outside of  $\text{Fe}_3\text{O}_4$  nanoparticles to encapsulate near-infrared fluorescent dyes and drug molecules. These multifunctional nanoparticles have MRI and fluorescence imaging capabilities and are promising candidates for magnetic field-controlled drug delivery.

Nanoparticle heterostructures are also useful for imaging. For example, Sun and colleagues (120) used gold- $\text{Fe}_3\text{O}_4$  dumbbell-shaped nanoparticles as dual optical/MRI agents. The heterostructured particles were synthesized through the use of  $\text{Fe}_3\text{O}_4$  nanoparticles as seeds for the growth of gold nanoparticles. In this approach, a single gold nanoparticle was physisorbed to the magnetic nanoparticle surface. The resulting heterostructure retained the magnetic properties



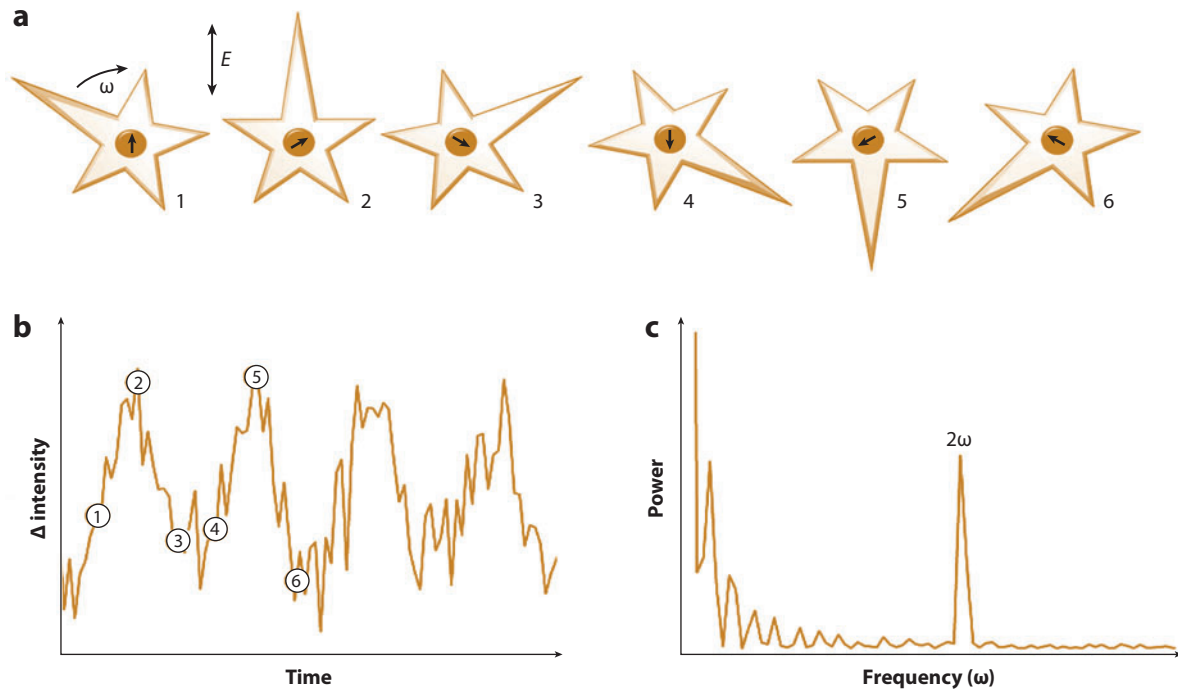


**Figure 8**

Dynamic optical contrast on gyromagnetic scattering. (a) Schematic of a gold nanostar with a near-infrared-active arm and a superparamagnetic core in various positions during gyration in response to a rotating magnetic field with frequency  $\omega$ . (b) Time-intensity plot of polarized scattering from a magnetic nanostar rotating at frequency  $\omega$  (two cycles), with reference to positions 1–6. (c) Power spectrum of gyromagnetic scattering (15 cycles). Reproduced with permission from Reference 122. Copyright 2009, American Chemical Society.

of  $\text{Fe}_3\text{O}_4$  and the plasmonic properties of gold nanoparticles and was used for both magnetic resonance contrast and an optical probe with confocal microscopy during *in vitro* studies of epithelial cells. The dumbbell structure does not suffer from fast signal loss and has a low limit of detection, which is likely to be advantageous compared with single nanoparticle agents.

Gao et al. (121) synthesized a core-shell nanoparticle made of  $\text{FePt}@\text{Fe}_2\text{O}_3$  with promising dual functionality of cytotoxicity and MRI capability. These nanoparticles were synthesized through the use of 3-nm-diameter FePt nanoparticles as seeds for the growth of a 3-nm-thick porous  $\text{Fe}_2\text{O}_3$  shell. This porous shell allowed slow diffusion of Pt atoms out of the core and resulted in the nanoparticles' cytotoxicity. Gao et al. proposed to use these nanoparticles to target and kill cancer cells while monitoring treatment via MRI.

The Wei group (122, 123) used a gold-coated  $\text{Fe}_3\text{O}_4$  core to make a superparamagnetic nanostar (**Figure 8**). The resulting particles integrated a polarization-sensitive plasmonic material with a magnetic material, yielding a nanostructure for use in gyromagnetic imaging. The plasmonic signal of the nanostars was modulated by a rotating magnetic field (123). Gyromagnetic imaging is useful because the electromagnetic signal depends on the frequency of the applied magnetic rotation, and the frequency-modulated signal can be transformed into a Fourier domain to improve the signal-to-noise ratio. The loss of signal and the high background noise in biological media can be overcome by the use of gyromagnetic imaging with nanostars; this technique has been used to image tumor cells (123).

## 6. CONCLUSIONS

The integration of magnetic nanoparticles with analytical methods has opened new avenues for sensing, purification, and quantitative analysis. The use of magnetic fields to control the motion and properties of magnetic nanoparticles is a tool for manipulating and analyzing species at the molecular level and has led to applications including analyte manipulation, chemical sensors, and imaging techniques. Magnetic nanoparticles uniquely combine superparamagnetic behavior with dimensions that are smaller than or on the same length scale as biomolecular structures; these characteristics have given rise to opportunities for bioanalysis that would not otherwise be possible. For example, heterofunctionalized nanoparticles or particle heterostructures can provide multiple analytical probes within the same nanoscale vehicle. Although there have been several investigations of such structures, in the future this area will surely witness significant growth and an increased impact on separation science and analysis.

## DISCLOSURE STATEMENT

The authors are not aware of any affiliations, memberships, funding, or financial holdings that might be perceived as affecting the objectivity of this review.

## LITERATURE CITED

1. Gu H, Xu K, Xu C, Xu B. 2006. Biofunctional magnetic nanoparticles for protein separation and pathogen detection. *Chem Commun.* 2006:941–49
2. Sun S, Zeng H, Robinson DB, Raoux S, Rice PM, et al. 2004. Monodisperse  $MFe_2O_4$  ( $M = Fe, Co, Mn$ ) nanoparticles. *J. Am. Chem. Soc.* 126:279
3. Hyeon T, Lee SS, Park J, Chung Y, Na HB. 2001. Synthesis of highly crystalline and monodisperse maghemite nanocrystallites with a size-selection process. *J. Am. Chem. Soc.* 123:12798–801
4. Park J, An K, Hwang Y, Park J, Noh H, et al. 2004. Ultra-large-scale syntheses of monodisperse nanocrystals. *Nat. Mater.* 3:891–95
5. Park J, Lee E, Hwang NM, Kang MS, Kim SC, et al. 2005. One-nanometer-scale size-controlled synthesis of monodisperse magnetic iron oxide nanoparticles. *Angew. Chem. Int. Ed.* 44:2872–77
6. Bao N, Shen L, Wang Y, Padhan P, Gupta A. 2007. A facile thermolysis route to monodisperse ferrite nanocrystals. *J. Am. Chem. Soc.* 129:12374–75
7. Bao N, Shen L, An W, Padhan P, Turner CH, Gupta A. 2009. Formation mechanism and shape control of monodisperse magnetic  $CoFe_2O_4$  nanocrystals. *Chem. Mater.* 21:3458–68
8. Chem M, Liu JP, Sun S. 2004. One-step synthesis of FePt nanoparticles with tunable size. *J. Am. Chem. Soc.* 126:8394–95
9. Figuerola A, Fiore A, Corato RD, Falqui A, Giannini C, et al. 2008. One-pot synthesis and characterization of size-controlled bimagnetic FePt–iron oxide heterodimer nanocrystals. *J. Am. Chem. Soc.* 130:1477–87
10. Lu A, Salabas EL, Schuh F. 2007. Magnetic nanoparticles: synthesis, protection, functionalization, and application. *Angew. Chem. Int. Ed.* 46:1222–44
11. Dave SR, Gao X. 2009. Monodisperse magnetic nanoparticles for biodetection, imaging, and drug delivery: a versatile and evolving technology. *Nanomed. Nanobiotechnol.* 1:583–609
12. Frey NA, Peng S, Cheng K, Sun S. 2009. Magnetic nanoparticles: synthesis, functionalization, and applications in bioimaging and magnetic energy storage. *Chem. Soc. Rev.* 38:2532–42
13. Hyeon T. 2003. Chemical synthesis of magnetic nanoparticles. *Chem. Commun.* 2003:927–34
14. Serna CJ, Veintemillas-Verdaguer S, Gonzalez-Carreño T, Morales MP, Tartaj P. 2005. Advances in magnetic nanoparticles for biotechnology applications. *J. Magn. Magn. Mater.* 290–291:28–34
15. Sahoo Y, Goodarzi A, Swihart MT, Ohulchanskyy TY, Kaur N, et al. 2005. Aqueous ferrofluid of magnetite nanoparticles: fluorescence labeling and magnetophoretic control. *J. Phys. Chem.* 109:3879–85

16. Kohler N, Fryxell GE, Zhang M. 2004. A bifunctional poly(ethylene glycol) silane immobilized on metallic oxide-based nanoparticles for conjugation with cell targeting agents. *J. Am. Chem. Soc.* 126:7206–11
17. Xu C, Xu K, Gu H, Zheng R, Liu H, et al. 2004. Dopamine as a robust anchor to immobilize functional molecules on the iron oxide shell of magnetic nanoparticles. *J. Am. Chem. Soc.* 126:9938–39
18. Grancharov SG, Zeng H, Sun S, Wang SX, O'Brien S, et al. 2005. Bio-functionalization of monodisperse magnetic nanoparticles and their use as biomolecular labels in a magnetic tunnel junction based sensor. *J. Phys. Chem. B* 109:13030–35
19. Dubertret B, Shourides P, Norris DJ, Noireaux V, Brivanlou AH, Libchaber A. 2002. In vivo imaging of quantum dots encapsulated in phospholipid micelles. *Science* 298:1759–62
20. Ban Z, Barnakov YA, Li F, Golub VO, O'Connor CJ. 2005. The synthesis of core-shell iron@gold nanoparticles and their characterization. *J. Mater. Chem.* 15:4660–62
21. Lyon JL, Fleming DA, Stone MB, Schiffer P, Williams ME. 2004. Synthesis of Fe oxide core/Au shell nanoparticles by iterative hydroxylamine seeding. *Nano Lett.* 4:719–23
22. Stöber W, Fink A, Bohn EJ. 1968. Controlled growth of monodisperse silica spheres in the micron size range. *J. Colloid Interface Sci.* 26:62–69
23. Lu Y, Yin Y, Mayers BT, Xia Y. 2002. Modifying the surface properties of superparamagnetic iron oxide nanoparticles through a sol-gel approach. *Nano Lett.* 2:183–86
24. Baranauskas VV, Zalich MA, Saunders M, St. Pierre TG, Riffle JS. 2005. Poly(styrene-*b*-vinylphenoxyphthalonitrile)-cobalt complexes and their conversion to oxidatively stable cobalt nanoparticles. *Chem. Mater.* 17:5246–54
25. Sarkar P, Ghosh D, Bhattacharyay D, Setford SJ, Turner APF. 2008. Electrochemical immunoassay for free prostate specific antigen (f-PSA) using magnetic beads. *Electroanalysis* 20:1414–20
26. Pamme N, Manz A. On-chip free-flow magnetophoresis: continuous flow separation of magnetic particles and agglomerates. *Anal. Chem.* 76:7250–56
27. Gijs MAM. 2004. Magnetic bead handling on-chip: new opportunities for analytical applications. *Microfluid. Nanofluid.* 1:22–40
28. Dubus S, Gravel J, Le Drogoff B, Nobert P, Veres T, Bourdreau D. 2006. PCR-free DNA detection using a magnetic bead-supported polymeric transducer and microelectromagnetic traps. *Anal. Chem.* 78:4457–64
29. Huang L-S, Chien S-H, Lin P-C, Wang K-Y, Chou P-H, et al. 2006. Chapter 10. In *Nanomaterials for Cancer Diagnosis*, ed. SSR Kumar Challa, 7:338–76. New York: Wiley
30. Lin P, Tseng M, Su A, Chen Y, Lin C. 2007. Functionalized magnetic nanoparticles for small-molecule isolation, identification, and quantification. *Anal. Chem.* 79:3401–8
31. Chou P, Chen S, Liao H, Lin P, Her G, et al. 2005. Nanoprobe-based affinity mass spectrometry for selected protein profiling in human plasma. *Anal. Chem.* 77:5990–97
32. Lin P, Chou P, Chen S, Liao H, Wang K, et al. 2005. Ethylene glycol-protected magnetic nanoparticles for a multiplexed immunoassay in human plasma. *Small* 2:485–89
33. Liu J, Tsai P, Lee YC, Chen Y. 2008. Affinity capture of uropathogenic *Escherichia coli* using pigeon ovalbumin-bound Fe<sub>3</sub>O<sub>4</sub>@Al<sub>2</sub>O<sub>3</sub> magnetic nanoparticles. *Anal. Chem.* 80:5425–32
34. Li Y, Lin Y, Tsai P, Chen C, Chen W, Chen Y. 2007. Nitrilotriacetic acid-coated magnetic nanoparticles as affinity probes for enrichment of histidine-tagged proteins and phosphorylated peptides. *Anal. Chem.* 79:7519–25
35. Xie H, Zhen R, Wang B, Feng Y, Chen P, Hao J. 2010. Fe<sub>3</sub>O<sub>4</sub>/Au core/shell nanoparticles modified with Ni<sup>2+</sup>-nitrilotriacetic acid specific to histidine-tagged proteins. *J. Phys. Chem. C* 114:4825–30
36. Chen GD, Alberts CJ, Rodriguez W, Toner M. 2010. Concentration and purification of human immunodeficiency virus type 1 virions by microfluidic separation of superparamagnetic nanoparticles. *Anal. Chem.* 82:723–28
37. Soelberg SD, Stevens RC, Limaye AP, Furlong CE. 2009. Surface plasmon resonance detection using antibody-linked magnetic nanoparticles for analyte capture, purification, concentration, and signal amplification. *Anal. Chem.* 81:2357–63

38. Morales-Cid G, Fekete A, Simonet BM, Lehmann R, Cárdenas S, et al. 2010. In situ synthesis of magnetic multiwalled carbon nanotube composites for the clean-up of (fluoro)quinolones from human plasma prior to ultrahigh pressure liquid chromatography analysis. *Anal. Chem.* 82:2743–52
39. Ballesteros-Gómez A, Rubio S. 2009. Hemimicelles of alkyl carboxylates chemisorbed onto magnetic nanoparticles: study and application to the extraction of carcinogenic polycyclic aromatic hydrocarbons in environmental water samples. *Anal. Chem.* 81:9012–20
40. Šafaříková M, Šafařík I. 1999. Magnetic solid-phase extraction. *J. Magn. Magn. Mater.* 194:108–12
41. Šafaříková M, Lunackova P, Komarek K, Hubka T, Šafařík I. 2007. Preconcentration of middle oxythylated nonylphenols from water samples on magnetic solid phase. *J. Magn. Magn. Mater.* 311:405–8
42. Zhao X, Shi Y, Wang T, Cai Y, Jiang G. 2008. Preparation of silica-magnetite nanoparticle mixed hemimicelle sorbents for extraction of several typical phenolic compounds from environmental water samples. *J. Chromatogr. A* 1188:140–47
43. Bromberg L, Raduyk S, Hatton TA. 2009. Functional magnetic nanoparticles for biodefense and biological threat monitoring and surveillance. *Anal. Chem.* 81:5637–45
44. Nako R, Matuo Y, Mishima F, Taguchi T, Nishijima S. 2009. Study on magnetic separation of nanosized ferromagnetic particles. *J. Phys. Conf. Ser.* 156:012032
45. Latham AH, Freita RS, Schiffer P, Williams ME. 2005. Capillary magnetic field flow fractionation and analysis of magnetic nanoparticles. *Anal. Chem.* 77:5055–62
46. Beveridge JS, Stephens JR, Latham AH, Williams ME. 2009. Differential magnetic catch and release: analysis and separation of magnetic nanoparticles. *Anal. Chem.* 81:9618–24
47. Carpino F, Zborozski M, Williams PS. 2007. Quadropole magnetic field-flow fractionation: a novel technique for the characterization of magnetic nanoparticles. *J. Magn. Magn. Mater.* 311:383–87
48. Carpino F, Moore LR, Zborozski M, Chalmers JJ, Williams PS. 2005. Analysis of magnetic nanoparticles using quadropole magnetic field–flow fractionation. *J. Magn. Magn. Mater.* 293:546–52
49. Earhart CM, Wilson RJ, White RL, Pourmand N, Wang SX. 2009. Microfabricated magnetic sifter for high-throughput and high-gradient magnetic separation. *J. Magn. Magn. Mater.* 321:1436–39
50. Cotton GB, Eldredge HB. 2002. Nanolevel magnetic separation model considering flow limitations. *Sep. Sci. Technol.* 37:3755–79
51. Chen H, Kaminski MD, Rosengart AJ. 2008. 2D modeling and preliminary in vitro investigation of a prototype high gradient magnetic separator for biomedical applications. *Med. Eng. Phys.* 30:1–8
52. Chen H, Bockenfeld D, Rempfer D, Kaminski MD, Liu X, Rosengart AJ. 2008. Preliminary 3-D analysis of a high gradient magnetic separator for biomedical applications. *J. Magn. Magn. Mater.* 320:279–84
53. Moeser GD, Roach KA, Green WH, Laibinis PE, Hatton TA. 2004. High-gradient magnetic separation of coated magnetic nanoparticles. *AIChE J.* 50:2835–48
54. Ditsch A, Lindenmann S, Laibinis PE, Wang DIC, Hatton TA. 2005. High-gradient magnetic separation of magnetic nanoclusters. *Ind. Eng. Chem. Res.* 44:6824–36
55. Albon C, Weddemann A, Auge A, Meißner D, Rott K, et al. 2009. Number sensitive detection and direct imaging of dipolar coupled magnetic nanoparticles by tunnel magnetoresistive sensors. *Appl. Phys. Lett.* 95:163106
56. Grancharov SG, Zeng H, Sun S, Wang SX, O'Brien S, et al. 2005. Bio-functionalization of monodisperse magnetic nanoparticles and their use as biomolecular labels in a magnetic tunnel junction based sensor. *J. Phys. Chem. B* 109:13030–35
57. Shen W, Schrag BD, Carter MJ, Xiao G. 2008. Quantitative detection of DNA labeled with magnetic nanoparticles using arrays of MgO-based magnetic tunnel junction sensors. *Appl. Phys. Lett.* 93:033903
58. Baibich MN, Broto JM, Fert A, Van Dau FN, Petroff F, et al. 1988. Giant magnetoresistance of (001)Fe/(001)Cr magnetic superlattices. *Phys. Rev. Lett.* 61:2472–75
59. Binasch G, Grünberg P, Saurenbach F, Zinn W. 1989. Enhanced magnetoresistance in layered magnetic structures with antiferromagnetic interlayer exchange. *Phys. Rev. B* 39:4828–30
60. Li G, Sun S, Wilson RJ, White RL, Pourmand N, Wang SX. 2006. Spin valve sensors for ultrasensitive detection of superparamagnetic nanoparticles for biological applications. *Sens. Actuators A* 126:98–106
61. de Boer BM, Kahlman JAHM, Jansen TPGH, Duric H, Veen J. 2007. An integrated and sensitive detection platform for magneto-resistive biosensors. *Biosens. Bioelectron.* 22:2366–70

62. Xu L, Yu H, Han S, Osterfeld S, White RL, et al. 2008. Giant magnetoresistive sensors for DNA microarray. *IEEE Trans. Magn.* 44:3989–91
63. Xu L, Yu H, Akhras MS, Han S, Osterfeld S, et al. 2008. Giant magnetoresistive biochip for DNA detection and HPV genotyping. *Biosens. Bioelectron.* 24:99–103
64. Wang AX, Li G. 2008. Advances in giant magnetoresistance biosensors with magnetic nanoparticle tags review and outlook. *IEEE Trans. Magn.* 44:1687–88
65. Hirsch R, Katz E, Willner I. 2000. Magneto-switchable bioelectrocatalysis. *J. Am. Chem. Soc.* 122:12053–54
66. Katz E, Sheeney-Haj-Ichia L, Basnar B, Felner I, Willner I. 2004. Magnetoswitchable controlled hydrophilicity/hydrophobicity of electrode surfaces using alkyl-chain-functionalized magnetic particles: application for switchable electrochemistry. *Langmuir* 20:9714–19
67. Katz E, Baron R, Willner I. 2005. Magnetoswitchable electrochemistry gated by alkyl-chain-functionalized magnetic nanoparticles: control of diffusional and surface-coated electrochemical processes. *J. Am. Chem. Soc.* 127:4060–70
68. Katz E, Willner I. 2005. Switching of directions of bioelectrocatalytic currents and photocurrents at electrode surfaces by using hydrophobic magnetic nanoparticles. *Angew. Chem. Int. Ed.* 44:4791–94
69. Katz E, Weizmann Y, Willner I. 2005. Magnetoswitchable reactions of DNA monolayers on electrodes: gating the processes by hydrophobic magnetic nanoparticles. *J. Am. Chem. Soc.* 127:9191–200
70. Zhu X, Han K, Li G. 2006. Magnetic nanoparticles applied in electrochemical detection of controllable DNA hybridization. *Anal. Chem.* 78:2447–49
71. Liu Z, Liu Y, Yang H, Yang Y, Shen G, Yu R. 2005. A phenol biosensor based on immobilizing tyrosinase to modified core-shell magnetic nanoparticles supported at a carbon paste electrode. *Anal. Chim. Acta* 533:3–9
72. Li J, Wei X, Yuan Y. 2009. Synthesis of magnetic nanoparticles composed by Prussian Blue and glucose oxidase for preparing highly sensitive and selective glucose biosensor. *Sens. Actuators B* 139:400–6
73. Liu Z, Yang H, Li Y, Liu Y, Li G, et al. 2006. Core-shell magnetic nanoparticles applied for immobilization of antibody on carbon paste electrode and amperometric immunosensing. *Sens. Actuators B* 113:956–62
74. Li J, Gao H. 2008. A renewable potentiometric immunosensor based on Fe<sub>3</sub>O<sub>4</sub> nanoparticles immobilized anti-IgG. *Electroanalysis* 20:881–87
75. Yantasee W, Hongsirikarn K, Warner CL, Choi D, Sangvanich T, et al. 2008. Direct detection of Pb in urine and Cd, Pb, Cu, and Ag in natural waters using electrochemical sensors immobilized with DMSA functionalized magnetic nanoparticles. *Analyst* 133:348–55
76. Tang D, Su B, Tang J, Ren J, Chen G. 2010. Nanoparticle-based sandwich electrochemical immunoassay for carbohydrate antigen 125 with signal enhancement using enzyme coated nanometer-sized enzyme-doped silica beads. *Anal. Chem.* 82:1527–34
77. Pan J, Yang Q. 2007. Antibody-functionalized magnetic nanoparticles for the detection of carcinoembryonic antigen using a flow-injection electrochemical device. *Anal. Bioanal. Chem.* 388:279–86
78. Huang H, Liu X, Zhang X, Liu W, Su X, Zhang Z. 2010. Fabrication of new magnetic nanoparticles (Fe<sub>3</sub>O<sub>4</sub>) grafted multiwall carbon nanotubes and heterocyclic compound modified electrode for electrochemical sensor. *Electroanalysis* 22:433–38
79. Baby TT, Ramaprabhu S. 2010. SiO<sub>2</sub> coated Fe<sub>3</sub>O<sub>4</sub> magnetic nanoparticle dispersed multiwalled carbon nanotubes based amperometric glucose biosensor. *Talanta* 80:2016–22
80. Cheng G, Zhao J, Tu Y, He P, Fang Y. 2005. A sensitive DNA electrochemical biosensor based on magnetite with a glassy carbon electrode modified by multi-walled carbon nanotubes in polypyrrole. *Anal. Chim. Acta* 533:11–16
81. Li J, Yuan R, Chai Y, Che X. 2010. Fabrication of a novel glucose biosensor based on Pt nanoparticles-decorated iron oxide-multiwalled carbon nanotubes magnetic composite. *J. Mol. Catal. B* 66:8–14
82. Tandon RP, Tripathy MR, Arora AK, Hotchandani S. 2006. Gas and humidity response of iron oxide-polypyrrole nanocomposites. *Sens. Actuators B* 114:768–73
83. Zhang J, Thurber A, Hanna C, Punnoose A. 2010. Highly shape-selective synthesis, silica coating, self assembly, and magnetic hydrogen sensing of hematite nanoparticles. *Langmuir* 26:5273–78

84. Ai Z, Deng K, Wan Q, Zhang L, Lee S. 2010. Facile microwave-assisted synthesis and magnetic and gas sensing properties of Fe<sub>3</sub>O<sub>4</sub> nanoroses. *J. Phys. Chem. C* 114:6237–42
85. Gao L, Zhuang J, Nie L, Zhang J, Zhang Y, et al. 2007. Intrinsic peroxidase-like activity of ferromagnetic nanoparticles. *Nat. Nanotechnol.* 2:577–83
86. Wei H, Wang E. 2008. Fe<sub>3</sub>O<sub>4</sub> magnetic nanoparticles as peroxidase mimetics and their applications in H<sub>2</sub>O<sub>2</sub> and glucose detection. *Anal. Chem.* 80:2250–54
87. Ding N, Yan N, Ren C, Chen X. 2010. Colorimetric determination of melamine in dairy products by Fe<sub>3</sub>O<sub>4</sub> magnetic nanoparticles–H<sub>2</sub>O<sub>2</sub>–ABTS detection system. *Anal. Chem.* 82:5897–99
88. Tsai HY, Hsu CF, Chiu IW, Fuh CB. 2007. Detection of C-reactive protein based on immunoassay using antibody-conjugated magnetic nanoparticles. *Anal. Chem.* 79:8416–19
89. Aurich K, Nagel S, Glöckl G, Weitschies W. 2007. Determination of the magneto-optical relaxation of magnetic nanoparticles as a homogenous immunoassay. *Anal. Chem.* 79:580–86
90. Wang J, Munir A, Zhu Z, Zhou HS. 2010. Magnetic nanoparticle enhanced surface plasmon resonance sensing and its application for the ultrasensitive detection of magnetic nanoparticle-enriched small molecules. *Anal. Chem.* 82:6782–89
91. Jun B, Noh MS, Kim J, Kim G, Kang H, et al. 2010. Multifunctional silver-embedded magnetic nanoparticles as SERS nanoprobes and their applications. *Small* 6:119–25
92. Noh MS, Jun B, Kim S, Kang H, Woo M, et al. 2009. Magnetic surface enhanced Raman spectroscopic (M-SERS) dots for the identification of bronchioalveolar stem cells in normal and lung cancer mice. *Biomaterials* 30:3915–25
93. Li J, He X, Wu Z, Wang K, Shen G, Yu R. 2003. Piezoelectric immunosensor based on magnetic nanoparticles with simple immobilization procedures. *Anal. Chim. Acta* 481:191–98
94. Lee H, Sun E, Ham D, Weissleder R. 2008. Chip-NMR biosensor for detection and molecular analysis of cells. *Nat. Med.* 14:869–75
95. Lee H, Yoon T, Figueiredo J, Swirski FK, Weissleder R. 2009. Rapid detection and profiling of cancer cells in fine-needle aspirates. *Proc. Natl. Acad. Sci. USA* 106:12459–64
96. Haun JB, Yoon T, Lee H, Weissleder R. 2010. Magnetic nanoparticle biosensors. *Nanomed. Nanobiotechnol.* 2:291–304
97. Xie J, Huang J, Li X, Sun S, Chen X. 2009. Iron oxide nanoparticle platform for biomedical applications. *Curr. Med. Chem.* 16:1278–94
98. Johnson GA, Benveniste H, Black RD, Hedlund LW, Maronpot RR, Smith BR. 1993. Histology by magnetic resonance microscopy. *Magn. Reson. Q.* 9:1–30
99. Josephson L, Tung C, Moore A, Weissleder R. 1999. High-efficiency intracellular magnetic labeling with novel superparamagnetic–Tat peptide conjugates. *Bioconjug. Chem.* 10:186–91
100. Weissleder R, Moore A, Mahmood U, Bhorade R, Benveniste H, et al. 2000. In vivo magnetic resonance imaging of transgene expression. *Nat. Med.* 6:351–54
101. Bulte JW, Zhang SC, van Gelderen P, Herynek V, Jordan EK, et al. 1999. Neurotransplantation of magnetically labeled oligodendrocyte progenitors: magnetic resonance tracking of cell migration and myelination. *Proc. Natl. Acad. Sci. USA* 96:15256–61
102. Hultman KL, Raffo AJ, Grzenda AL, Harris PE, Brown TR, O'Brien S. 2008. Magnetic resonance imaging of major histocompatibility class II expression in the renal medulla using immunotargeted superparamagnetic iron oxide nanoparticles. *Am. Chem. Soc. Nano* 2:477–84
103. El-Boubbou K, Zhu DC, Vasileiou C, Borhan B, Prosperi D, et al. 2010. Magnetic glyco-nanoparticles: a tool to detect, differentiate, and unlock the glyco-codes of cancer via magnetic resonance imaging. *J. Am. Chem. Soc.* 132:4490–99
104. Zhao M, Beauregard DA, Loizou L, Davletov B, Brindle KM. 2001. Non-invasive detection of apoptosis using magnetic resonance imaging and targeted contrast agent. *Nat. Med.* 7:1241–44
105. Tromsdorf UI, Bigall NC, Kaul MG, Bruns OT, Nikolic MS, et al. 2007. Size and surface effects of the MRI relaxivity of manganese ferrite nanoparticle contrast agents. *Nano Lett.* 7:2422–27
106. Bruns OT, Itrich H, Peldschus K, Kaul MG, Tromsdorf UI, et al. 2009. Real-time magnetic resonance imaging and quantification of lipoprotein metabolism in vivo using nanocrystals. *Nat. Nanotechnol.* 4:193–200

107. Bae KH, Kim YB, Lee Y, Hwang JY, Park HW, Park TG. 2010. Bioinspired synthesis and characterization of gadolinium-labeled magnetite nanoparticles for dual contrast  $T_1$ - and  $T_2$ -weighted magnetic resonance imaging. *Bioconjug. Chem.* 21:505–12
108. Judenhofer MS, Wehrl HF, Newport DF, Catana C, Siegel SB, et al. 2008. Simultaneous PET-MRI: a new approach for functional and morphological imaging. *Nat. Med.* 14:459–65
109. Glaus C, Rossin R, Welch MJ, Bao G. 2010. In vivo evaluation of  $^{64}\text{Cu}$ -labeled magnetic nanoparticles as a dual-modality PET/MR imaging agent. *Bioconjug. Chem.* 21:715–22
110. Lee HY, Li Z, Chen K, Hsu AR, Xu C, et al. 2008. PET/MRI dual-modality tumor imaging using arginine-glycine-aspartic (RGD)-conjugated radiolabeled iron oxide nanoparticles. *J. Nucl. Med.* 49:1371–79
111. Jarett BR, Gustafsson B, Kukis DL, Louie AY. 2008. Synthesis of  $^{64}\text{Cu}$ -labeled magnetic nanoparticles for multimodal imaging. *Bioconjug. Chem.* 19:1496–504
112. Choi JS, Park JC, Nah H, Woo S, Oh J, et al. 2008. A hybrid nanoparticle probe for dual-modality positron emission tomography and magnetic resonance imaging. *Angew. Chem. Int. Ed.* 47:6259–62
113. Foy SP, Manthe RL, Foy ST, Dimitrijevic S, Krishnamurthy N, Labhasetwar V. 2010. Optical imaging and magnetic field targeting of magnetic nanoparticles in tumors. *Am. Chem. Soc. Nano* 4:5217–24
114. Cheng FY, Wang SPH, Su CH, Tsai TL, Wu PC, et al. 2008. Stabilizer-free poly(lactide-co-glycolide) nanoparticles for multimodal biomedical probes. *Biomaterials* 29:2104
115. Nitin N, LaConte LEW, Zurkiya O, Hu X, Bao G. 2004. Functionalization and peptide-based delivery of magnetic nanoparticles as an intracellular MRI contrast agent. *J. Biol. Inorg. Chem.* 9:706–12
116. Xie J, Chen K, Huang J, Lee S, Wnag J, et al. 2010. PET/NIRF/MRI triple functional iron oxide nanoparticles. *Biomaterials* 31:3016–22
117. Veisoh O, Sun C, Gunn J, Kohler N, Gabikian P, et al. 2005. Optical and MRI multifunctional nanoprobe for targeting gliomas. *Nano Lett.* 5:1003–8
118. Liong M, Lu J, Kovochich M, Xia T, Ruehm SG, et al. 2008. Multifunctional inorganic nanoparticles for imaging, targeting, and drug delivery. *Am. Chem. Soc. Nano* 2:889–96
119. Santra S, Kaittanis C, Grimm J, Perez JM. 2009. Drug/dye-loaded, multifunctional iron oxide nanoparticles for combined targeted cancer therapy and dual optical/magnetic resonance imaging. *Small* 5:1862–68
120. Xu C, Xie J, Ho D, Wang C, Kohler N, et al. 2008. Au- $\text{Fe}_3\text{O}_4$  dumbbell nanoparticles as dual-functional probes. *Angew. Chem. Int. Ed.* 47:173–76
121. Gao J, Liang G, Cheung JS, Pan Y, Kuang Y, et al. 2008. Multifunctional yolk-shell nanoparticles: a potential MRI contrast and anticancer agent. *J. Am. Chem. Soc.* 130:11828–33
122. Wei Q, Song H, Leonov AP, Hale JA, Oh D, et al. 2009. Gyromagnetic imaging: dynamic optical contrast using nanostars with magnetic cores. *J. Am. Chem. Soc.* 131:9728–34
123. Song H, Wie Q, Ong QK, Wei A. 2010. Plasmon-resonant nanoparticles and nanostars with magnetic cores: synthesis and magnetomotive imaging. *Am. Chem. Soc. Nano* 4:5163–73



# Contents

A Century of Progress in Molecular Mass Spectrometry <i>Fred W. McLafferty</i> .....	1
Modeling the Structure and Composition of Nanoparticles by Extended X-Ray Absorption Fine-Structure Spectroscopy <i>Anatoly I. Frenkel, Aaron Yevick, Chana Cooper, and Relja Vasic</i> .....	23
Adsorption Microcalorimetry: Recent Advances in Instrumentation and Application <i>Matthew C. Crowe and Charles T. Campbell</i> .....	41
Microfluidics Using Spatially Defined Arrays of Droplets in One, Two, and Three Dimensions <i>Rebecca R. Pompano, Weishan Liu, Wenbin Du, and Rustem F. Ismagilov</i> .....	59
Soft Landing of Complex Molecules on Surfaces <i>Grant E. Johnson, Qichi Hu, and Julia Laskin</i> .....	83
Metal Ion Sensors Based on DNAszymes and Related DNA Molecules <i>Xiao-Bing Zhang, Rong-Mei Kong, and Yi Lu</i> .....	105
Shell-Isolated Nanoparticle-Enhanced Raman Spectroscopy: Expanding the Versatility of Surface-Enhanced Raman Scattering <i>Jason R. Anema, Jian-Feng Li, Zhi-Lin Yang, Bin Ren, and Zhong-Qun Tian</i> .....	129
High-Throughput Biosensors for Multiplexed Food-Borne Pathogen Detection <i>Andrew G. Gebring and Shu-I Tu</i> .....	151
Analytical Chemistry in Molecular Electronics <i>Adam Johan Bergren and Richard L. McCreery</i> .....	173
Monolithic Phases for Ion Chromatography <i>Anna Nordborg, Emily F. Hilder, and Paul R. Haddad</i> .....	197
Small-Volume Nuclear Magnetic Resonance Spectroscopy <i>Raluca M. Fratila and Aldrik H. Velders</i> .....	227



The Use of Magnetic Nanoparticles in Analytical Chemistry <i>Jacob S. Beveridge, Jason R. Stephens, and Mary Elizabeth Williams</i> .....	251
Controlling Mass Transport in Microfluidic Devices <i>Jason S. Kuo and Daniel T. Chiu</i> .....	275
Bioluminescence and Its Impact on Bioanalysis <i>Daniel Scott, Emre Dikici, Mark Ensor, and Sylvia Daunert</i> .....	297
Transport and Sensing in Nanofluidic Devices <i>Kaimeng Zhou, John M. Perry, and Stephen C. Jacobson</i> .....	321
Vibrational Spectroscopy of Biomembranes <i>Zachary D. Schultz and Ira W. Levin</i> .....	343
New Technologies for Glycomic Analysis: Toward a Systematic Understanding of the Glycome <i>John F. Rakus and Lara K. Mahal</i> .....	367
The Asphaltenes <i>Oliver C. Mullins</i> .....	393
Second-Order Nonlinear Optical Imaging of Chiral Crystals <i>David J. Kissick, Debbie Wanapun, and Garth J. Simpson</i> .....	419
Heparin Characterization: Challenges and Solutions <i>Christopher J. Jones, Szabolcs Beni, John F.K. Limtiaco, Derek J. Langeslay, and Cynthia K. Larive</i> .....	439

## Indexes

Cumulative Index of Contributing Authors, Volumes 1–4 .....	467
Cumulative Index of Chapter Titles, Volumes 1–4 .....	470

## Errata

An online log of corrections to the *Annual Review of Analytical Chemistry* articles may be found at <http://arjournals.annualreviews.org/errata/anchem>